



Correlation between PSD and adsorption of anionic dyes with different molecular weights on activated carbon



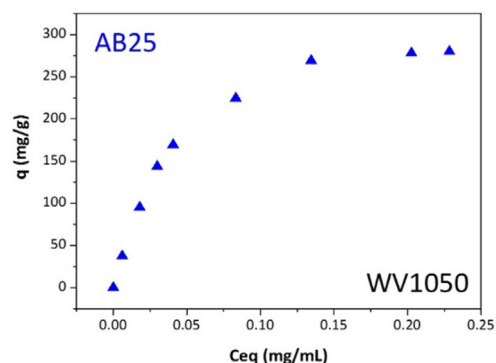
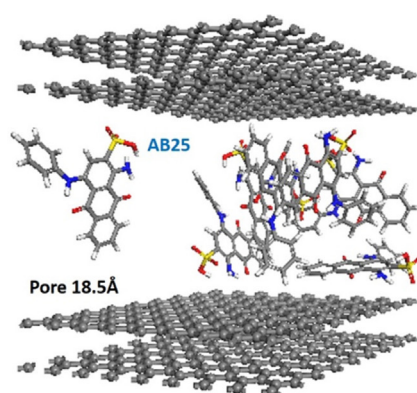
J.E. Aguiar, J.C.A. de Oliveira, P.F.G. Silvino, J.A. Neto, I.J. Silva Jr., S.M.P. Lucena*

Universidade Federal do Ceará, Centro de Tecnologia, Departamento de Engenharia Química, Grupo de Pesquisa em Separações por Adsorção—GPSA, Campus do Pici, Bloco 709, CEP 60455-760 Fortaleza, CE, Brazil

HIGHLIGHTS

- There is a strong correlation between anionic dye adsorption capacity and the pore size distribution of the commercial activated carbons.
- Dye chemistry impact in the retention capacity if the molecular specie is prone to form agglomerates.
- The use of N₂ derived PSD and molecular simulation in the NVT ensemble can be a useful tool to best match a dye to an activated carbon.

GRAPHICAL ABSTRACT



ARTICLE INFO

Article history:

Received 12 August 2015
 Received in revised form 26 August 2015
 Accepted 21 September 2015
 Available online 25 September 2015

Keywords:

Dyes
 Adsorption
 Activated Carbon
 Molecular Simulation
 PSD

ABSTRACT

The correlation between the adsorption capacity of commercial activated carbons and the pore size distributions in the removal of anionic dyes was investigated. We performed experimental adsorption isotherms measurements of the anionic dyes reactive red 120 (RR120), procion red MX-5B (PRMX-5B) and acid blue 25 (AB-25) in the activated carbons WV1050, Norit R1 and Maxsorb. The activated carbons were carefully characterized by N₂ adsorption at 77 K and molecular simulation methods to obtain the PSDs and retention capacity of selected pores (8.9, 18.5 and 30.9 Å). Batch experiments were carried out in order to obtain single component dye isotherms. We found that the proposed selected pores of the PSD directly correlates with adsorption capacity when the size of the dye molecule is compatible with the carbon pore size. Between RR120 and PRMX-5B we noted that dye chemistry strongly affect the retention capacity. Based on our results, the use of N₂ derived PSD and molecular simulation of dye retention in selected pores can be a useful tool to guide to the optimization of carbon-based adsorbents for dye removal.

© 2015 Elsevier B.V. All rights reserved.

1. Introduction

Thousands of dyes are used for printing and dyeing industries generating potential pollutants. Dyes, even in low concentrations,

* Corresponding author. Fax: +55 85 3366 9601.
 E-mail address: smlucena@uol.com.br (S.M.P. Lucena).

affect the aquatic ecosystem. Some of them are carcinogenic and mutagenic. Hence, ways and means are required to remove the dyes from wastewater [1,2].

The industry currently uses adsorption on activated carbon for dye removal. The porous nature and the high surface area of this adsorbent material allows removal of anionic and cationic dyes. Adsorption also has a specific advantage of removing the complete dye molecule, unlike certain removal techniques that destroy only the dye chromophore, leaving the harmful residual moieties (metals) in the effluent [3].

Although researchers extensively investigated activated carbons from different sources aiming dye removal [4–7], most of these studies underestimate the importance of pore size distribution (PSD) of the carbon, interpreting the results in terms of surface chemistry. The lack of carbon PSD characterization is a consistent similarity among those papers. Few studies are dedicated to PSD contribution [8–11]. In Pelekani and Li studies [8–10], they investigated the adsorption of dyes in a series of activated carbon fiber (ACF). The ACFs were produced carefully so that the PSDs remain unimodal. In our opinion, the PSD is the controlling adsorbent property between dyes and the majority of activated carbon materials, even without uniform pore size distribution.

Our objective is to extend the pioneering study of Pelekani and Snoeyink [8] to commercial activated carbons produced from different raw materials and processes with irregular PSDs. We want to interpret essential dye adsorption results in activated carbons, as showed by isotherms, using PSD data. To attain that objective we choose 3 commercial activated carbon (Norit R1, WV1050 and MAXSORB) with different PSDs and 3 dyes molecules (acid blue 25; procion red MX5B and reactive red 120) with increasing sizes.

The amorphous nature of the activated carbon is one of the main limiting factors for obtaining reliable PSD. For this reason, Pelekani used activated carbon fibers with uniform porous structures. As we select commercial materials, the PSDs were carefully determined with a kernel of N₂ isotherms obtained by the Monte Carlo method, previously tested in other systems [12–14]. Although the known accessibility issues of N₂, experimental nitrogen isotherms dominate the literature of activated carbon studies and their PSD are very similar to Ar isotherms, a less reactive probe-gas [15,16]. To assist in the correlation between features of experimental isotherms and the PSD of activated carbons, molecular simulations in the NVT ensemble were performed. This enabled us to gain atomic level insights of the system dye/slit pore. These simulations helped confirm whether the dye molecule accesses certain pore size and the amount of dye that is necessary to saturate that pore. This study therefore, proposes a new methodology that combines experimental data and molecular simulation that is able to quantitatively describe those systems, as the non-availability of dye vapor pressure data, prevents calculations in the grand canonical ensemble.

2. Materials and methods

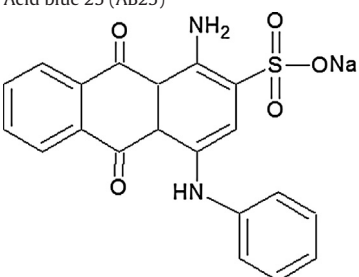
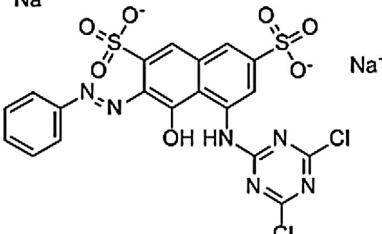
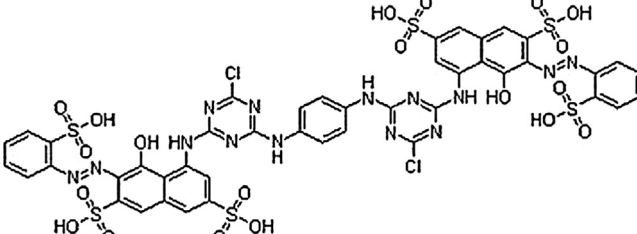
2.1. Materials

Reactive Red 120 (RR120), Procion Red MX5B (PRMX-5B) and Acid blue 25 (AB25) dyes were purchased from Sigma-Aldrich Chemical Co. (USA). Table 1 shows the chemical structure and their characteristics of these dyes. All dye solutions were prepared with distilled water.

Norit R1, Maxsorb and WV1050 activated carbon came from Norit Inc. (Netherlands), Kansai Coke and Chemicals (Japan) and MeadWestVaco (USA), respectively. Concerning raw material, WV1050 is wood-based, Norit R1 is bitumen-based and Maxsorb activated carbon is manufactured from petroleum coke.

Table 1

Structures and chemical characteristics of the dyes acid blue 25 (AB25), procion red MX-5B (PRMX-5B) and reactive red 120 (RR120).

Acid blue 25 (AB25)	
	
Molecular formula	C ₂₀ H ₁₃ N ₂ NaO ₅ S
Molar mass (g/mol)	416,38
λ _{max} (nm)	605
Procion red MX-5B (PRMX-5B)	
	
Molecular formula	C ₁₉ H ₁₀ Cl ₂ N ₆ Na ₂ O ₇ S ₂
Molar mass (g/mol)	615,33
λ _{max} (nm)	600
Reactive red 120 (RR120)	
	
Molecular formula	C ₄₄ Cl ₂ H ₂₄ N ₁₄ Na ₆ O ₂₀ S ₆
Molar mass (g/mol)	1469,98
λ _{max} (nm)	583

2.2. Textural properties of activated carbon

N₂ adsorption/desorption experiments at 77 K were performed to obtain reliable isotherms in order to determine textural properties. The isotherms were obtained in an automatic sorptometer Autosorb 1C (Quantachome, USA and Micromeritics, ASAP 2000) at low pressure. The specific surface area was calculated using the BET methodology and micropore volume was determined using the Dubinin–Radushkevich (DR) equation, according to the procedure described by various authors [17,18]. The total pore volume was obtained from the N₂ volume adsorbed at a relative pressure of 0.95.

2.3. Experimental adsorption isotherms

Batch adsorption experiments were performed at 22 °C (± 2 °C) in an orbital shaker (Tecnal TE-165, Brazil) at 30 rpm. 20 mL of dye solution were put in contact with 15 mg of activated carbon in 50 mL polyethylene flasks. At the end of experiments the supernatant were collected and centrifuged for 10 min at 10,000 rpm (refrigerated microcentrifuge Cientec CT – 15000R). The concentration of each dye in the supernatant solutions before and after the

adsorption experiments were determined in UV/Vis spectrophotometer (Thermo Scientific BioMate 3, USA) in order to obtain the equilibrium concentration of dye in liquid phase. A wavelength scanning for determination the maximum absorbance was performed. The maximum wavelength (λ_{max}) was observed at 605 nm for AB25, 583 for PRMX5R and 583 nm for RV120.

Several batch experiments were carried out in order to obtain the information about the equilibrium isotherms. For this aim, RV120, PRMX-5B and AB25 dye stock solutions were prepared in neutral pH. For the measurement of adsorption isotherms, different initial concentrations of each dye were put in contact with the adsorbent and after interval time necessary (2 h) to reach the equilibrium the supernatant was collected and centrifuged. Dye amount adsorbed in solid phase (specific relative surface excess of dye with respect to water, q^*) was calculated according to Eq. (1):

$$q^* = \frac{V(c_0 - c_{\text{eq}})}{m_{\text{ads}}} \quad (1)$$

where c_0 (mg/mL) and c_{eq} (mg/mL) are the initial and the final (equilibrium) concentration of dye in liquid phase, V (mL) is the volume of solution, and m_{ads} (g) is the dried-weight of activated carbon. All the adsorption experiments were performed twice.

2.4. Models

The dye molecules in their neutral form are minimized using DFT (LDA/PWC functional) using DMol3 module of material studio (Accelrys Inc.) and the atoms partial charges of the final minimized structure was retained to be used in the NVT simulations (Fig. 1).

The activated carbon pores was modeled with a slit-shaped simulation cell of $40 \text{ \AA} \times 40 \text{ \AA}$ with walls made of two layers of graphene sheets. The graphene sheets were made up of discrete atoms of carbon.

2.5. Carbon PSD determination

The PSD is computationally determined through the deconvolution of a kernel of simulated isotherms using an experimental probe-gas isotherm of nitrogen at 77.4 K.

The integral adsorption equation to obtain the PSD is expressed as follows:

$$Q(p)_{\text{EXP}} = \int q(p, H) \times f(H) dH \quad (2)$$

where $Q(p)_{\text{EXP}}$ is the experimental isotherm expressed as the total amount of adsorbate per gram of adsorbent at pressure p ; $q(p, H)$ represents the simulated local isotherms database (Kernel), obtained for pores with different sizes (H), expressed as total adsorbate uptake at pressure p per pore volume and $f(H)$ represents the PSD. Solving this equation consists of determining the best combination of local isotherms that would reproduce the experimental isotherm, and the term $f(H)$ denotes the weight of this combination. The pore size distribution is then obtained by solving the Eq. (2) numerically via a fast non-negative least square algorithm in combination with a method to stabilize the result [19–22]. Regularization was introduced based in the “L curve” criteria via a smoothing parameter (Fig. S9—Supporting information) [23,24]. This method is needed to stabilize the numerical computation, by incorporating additional constraints based on the smoothness of the PSD.

After determination of the complete PSD for each activated carbon, the pore series was approximated for three representative pore size (8.9, 18.5 and 27.9 Å). This approximation methodology have been tested and successfully reproduced the monocomponent and multicomponent isotherms of alkanes from C1 to C4 [12].

Table 2
Textural properties of the activated carbon from N2 isotherms.

Carbon sample	S_{BET} (m ² /g)	V_p (cm ³ /g)	V_μ (cm ³ /g)
NORIT R1	688	0.621	0.31
WV1050	1615	1.03	0.76
MAXSORB	3250	1.65	1.35

2.6. Simulation details

The 12 -6 Lennard-Jones potential was used to describe the fluid–fluid and solid–fluid interactions.

$$U(r_{ij}) = 4 \times \epsilon_{ij} \times \left[\left(\frac{\sigma_{ij}}{r_{ij}} \right)^{12} - \left(\frac{\sigma_{ij}}{r_{ij}} \right)^6 \right] + \frac{q_i q_j}{r_{ij}} \quad (2)$$

here, ϵ_{ij} is the well depth, σ_{ij} is the finite distance in which the energy of interaction is zero and r_{ij} is the distance between interacting atoms i and j . In the second term, q_i and q_j are point charges separated by the distance r_{ij} . The force-field parameters for the dye molecules were taken from Universal force-field [25]. Universal is a purely diagonal, harmonic forcefield. Bond stretching is described by a harmonic term, angle bending by a three-term Fourier cosine expansion, and torsions and inversions by cosine-Fourier expansion terms.

The electrostatic potential was calculated by Ewald method [26]. The atoms in the graphene sheet are treated with the Steele parameters, where $\epsilon = 0.055$ kcal/mol and $\sigma = 3.4 \text{ \AA}$ [27]. The cross terms were obtained through typical arithmetic and geometric combination rules.

The carbon pore was first tested for size compatibility with the dye molecule. Attempts to load molecules were done to each pore size. If we succeed, the pore was loaded with increased number of molecule using Monte Carlo algorithm in the canonical ensemble (NVT) to obtain the dye maximum density inside the pore. The NVT ensemble is the appropriated choice for conformational searches [28]. The sorbate molecules are random inserted in the simulation box until specified load has been reached. After that, two moves are performed: rotation and translation, until the system reach equilibrium. The Monte Carlo computations were done in the sorption module of materials studio (Accelrys Inc.). Between 4×10^6 and 6×10^6 Monte Carlo steps were performed. Plots with the minimized energies are presented in the Fig. S6 (Supporting information). The potential cut-off distance was 15.5 Å, and interactions between two atoms separated by distances less than 0.4 Å were ignored. We also did tests with increasing LJ cut-offs, until 19.5 Å, obtained similar results.

3. Result and discussion

3.1. Textural properties and PSD

Fig. 2 shows the experimental isotherms of N₂ at 77 K for the three carbons that we analyzed.

Based on the N2 isotherms, we infer that all three samples of activated carbons are different. The maximum adsorption of N2 decrease in the order Maxsorb > WV1050 > Norit R1. The area (S_{BET}), volume total of pores (V_p) and micropores volumes (V_μ) derived from N2 isotherm are shown in Table 2. The sample of Norit R1 has the lowest degree of activation and Maxsorb the highest degree of activation.

By applying the N2 kernel of simulated isotherms [12], we extracted the full PSD for the samples of Norit R1, WV1050 and Maxsorb (Fig. 3). The pore volumes assigned to each representative pore (8.9, 18.5 and 27.9 Å) were mapped with different colors.

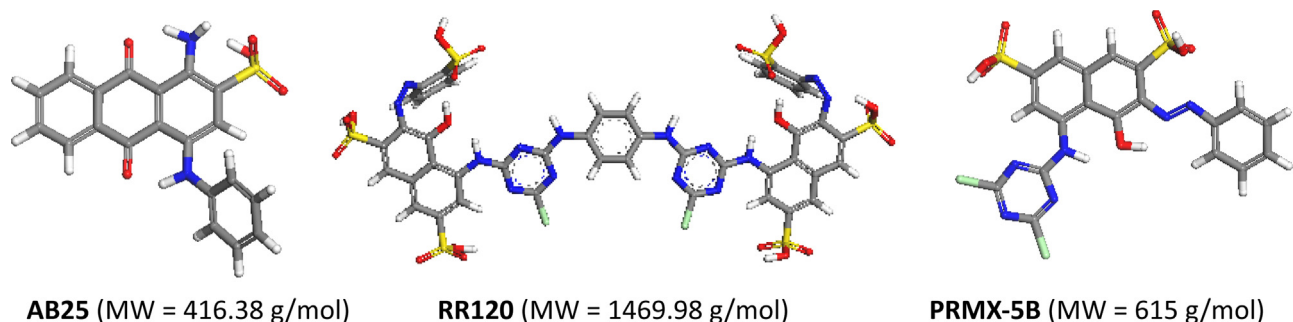


Fig. 1. Geometric representation of the dye molecules. Legend: sulfur-yellow, carbon-gray, nitrogen-blue, oxygen-red, hydrogen-white and chlorine-green. (For interpretation of the references to color in this figure legend, the reader is referred to the web version of this article.)

Also in the Fig. 3 are the percentages of the pore total volume of each sample associated with each pore size range. Activated carbon WV 1050 has the highest percentage of pores in the mesoporous range (20–50 Å) while the activated carbon Norit R1 has the highest percentage in the micropores range (<20 Å). The activated carbon Maxsorb has a more balanced distribution of pores in both micropore and mesopore ranges. Despite the activated carbon Maxsorb have presented a volume of pores far superior to the others activated carbons in the pore range from 8.9 to 18.5 Å, this volume would be even greater if a kernel with pores of one graphene layer was used. Bhatia and Nguyen [29–31] demonstrated that coals with higher surface areas also has a greater number of walls comprised of a single layer of graphene sheet, being described more accurately with these pore models. In general, when mixed layers models is used, a shift to narrower pores in the carbon PSD has been noted. A study of one layer wall impact on Maxsorb PSD regarding to the other carbons presented, despite being relevant, is beyond the scope of this study. We also highlight that the Maxsorb PSD presented follows the standard calculation methodology used by commercial gas sorption analyzers being consistent with experimental data from literature [32–34].

3.2. Experimental isotherms

Adsorption isotherms (specific relative surface excess) for RR120, PRMX-5B and AB25 on NORIT R1, MAXSORB and WV1050 activated carbon are shown in Fig. 4. The initial region of the isotherm follows the Henry's law for diluted dye concentration in liquid phase—a linear behavior. In this initial region, the amount adsorbed is very high for initial dye concentrations and the slope of the isotherm increase very fast. However, the slope of the isotherm decrease drastically as the dye concentration was increased reaching saturation. This is a typical behavior of favorable adsorption isotherm.

According to these results, the smallest dye AB25 presented the higher adsorption capacity followed by PRMX-5B and finally for RR120, the larger dye molecule.

3.3. Correlation between PSD and isotherms

When performing the compatibility test, we found that the dye RR120 did not match the 8.9 Å pore while the others dyes are compatible with this pore size. Although the RR120 dye be compatible with the 18.5 and 27.9 Å pores they rapidly reach saturation with only 1 and 3 molecules/800 Å², respectively. The PRMX-5B dye also rapidly fill the 8.9 Å pore (1 molecule/800 Å²). From the NVT simulation data, we compute the simulated maximum amount of dye in each pore, expressing this amount in mg of dye/volume of pore in cm³ (Table 3). From the PSD, we know the volumes of the rep-

Table 3

Simulated maximum amount (q_{\max}) of dye in each selected pore.

Pore size (Å)	AB25 mg/cm ³	PRMX-5B mg/cm ³	RR120 mg/cm ³
8.9	388	286	zero
18.5	653	690	329
27.9	804	915	655

Table 4

Pore volume (V_p) correlated with characteristic pores for each activated carbon.

Pore size (Å)	Norit R1 pore volume (cm ³ /g)	WV1050 pore volume (cm ³ /g)	Maxsorb pore volume (cm ³ /g)
8.9	0.25	0.12	0.25
18.5	0.27	0.28	0.72
27.9	0.09	0.74	0.69

Table 5

Theoretical maximum dye capacity (Q_{\max}) on each activated carbon. Unit: mg of dye/g of activated carbon.

	AB25 (mg/g)	PRMX-5B (mg/g)	RR120 (mg/g)
Norit			
8.9 Å	97	71	0
18.5 Å	176	186	89
27.9 Å	72	82	59
Q_{\max}	345	340	148
Exp.	118	85	31
WV1050			
8.9 Å	46	34	0
18.5 Å	183	193	92
27.9 Å	595	677	485
Q_{\max}	825	905	577
Exp.	191	142	33
Maxsorb			
8.9 Å	97	71	0
18.5 Å	470	496	237
27.9 Å	555	631	452
Q_{\max}	1123	1200	690
Exp.	288	162	35

representative pore for each activated carbon expressed in cm³/gram of the carbon (Table 4).

The theoretical maximum dye capacity (Q_{\max}) for each carbon is determined by the sum of the products of the volume of each pore (V_p) by the simulated maximum dye amount (q_{\max}) in each pore (Eq. (3) and Table 5).

$$Q_{\max} = \sum_{n=1}^N Vp_n \times q_{\max_n} \quad (3)$$

We also present in Table 5 the experimental maximum capacity as determined by the batch essays. As expected, the experimental

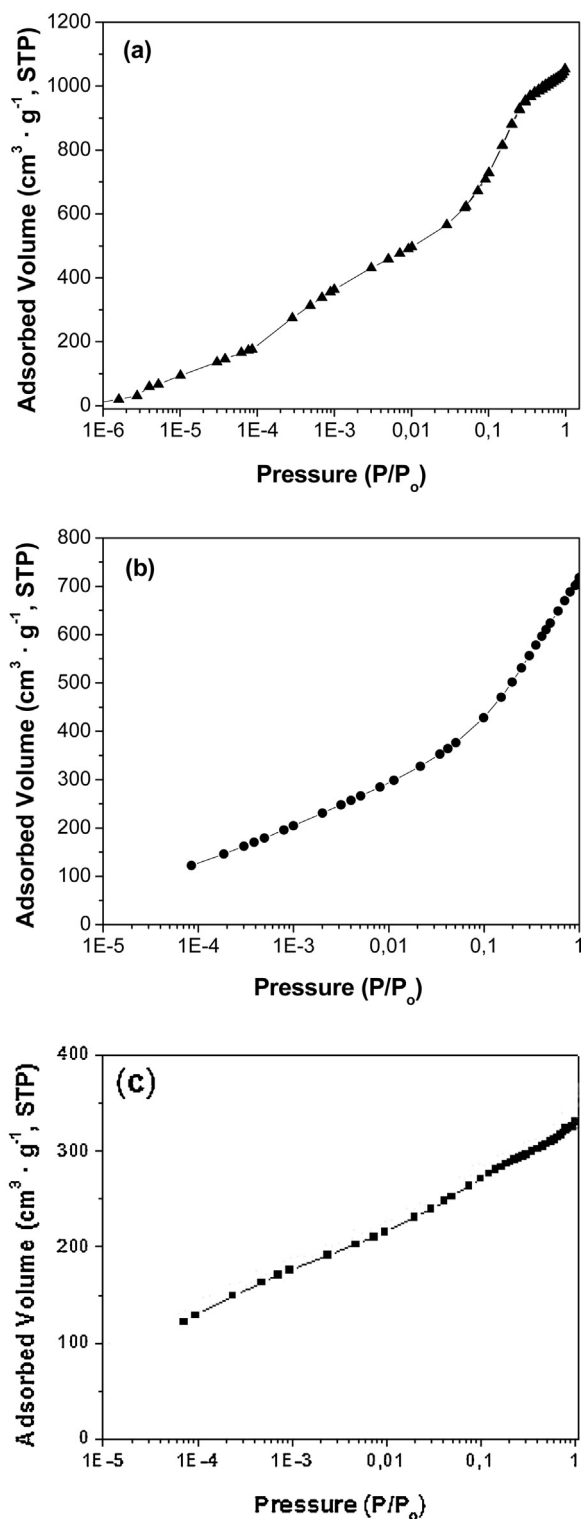


Fig. 2. Experimental N_2 isotherms and PSD for carbons Maxsorb (a), WV 1050 (b), Norit R1 (c).

maximum capacity is lower than the theoretical estimate. The NVT calculations did not consider any influence of the water, carbon pore network or cations in the solution. Even though, the simplified model still has correlation with the real system. For example, the NVT calculation showed that the activated carbon WV1050 retain almost two times the AB25 dye when comparing with Norit carbon. Indeed, we found that WV1050 adsorbs experimentally 190 mg/g and Norit adsorbs 118 mg/g.

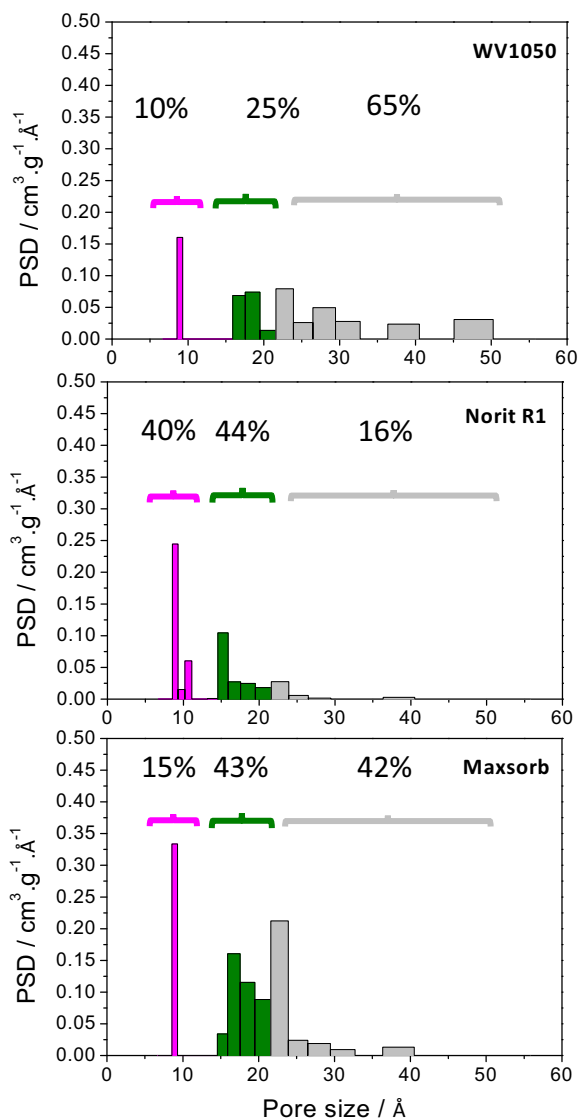


Fig. 3. PSD of (a) WV1050, (b) Norit R1 and (c) Maxsorb activated carbons calculated from the kernel of the N_2 isotherms obtained at 77.4 K [12]. The bars are colored according to the volume represented by each representative pore size (red, 8.9 Å; blue, 18.5 Å; gray, 27.9 Å). (For interpretation of the references to color in this figure legend, the reader is referred to the web version of this article.)

In order to correlate the theoretical data from PSD and the experimental results we will analyse each dye from the smallest (AB25) to the largest (RR120).

3.3.1. AB25

Despite the higher values obtained by simulation, the ratio of adsorbed amounts between the activated carbons are reasonably maintained. The theoretical data showed that Maxsorb and WV 1050 retain respectively, 3 and 2.3 times more dye than the Norit R1 carbon. Experimentally we found the ratio of adsorbed amount as 2.5 and 1.6 for Maxsorb:Norit and WV 1050:Norit respectively. Other experimental output that can be explained by PSD is the remarkable difference in the isotherm slope of the activated carbon Norit. We observe in Table 4 that the pore volume in the 8.9 Å range for Norit R1 is twice greater than that of the carbon WV 1050. Norit also has the same pore volume in the 18.5 Å range while the carbon WV 1050 has greater pore volume in the 27.9 Å range. Thus, the dye AB25 is readily adsorbed on Norit R1 carbon, which explains

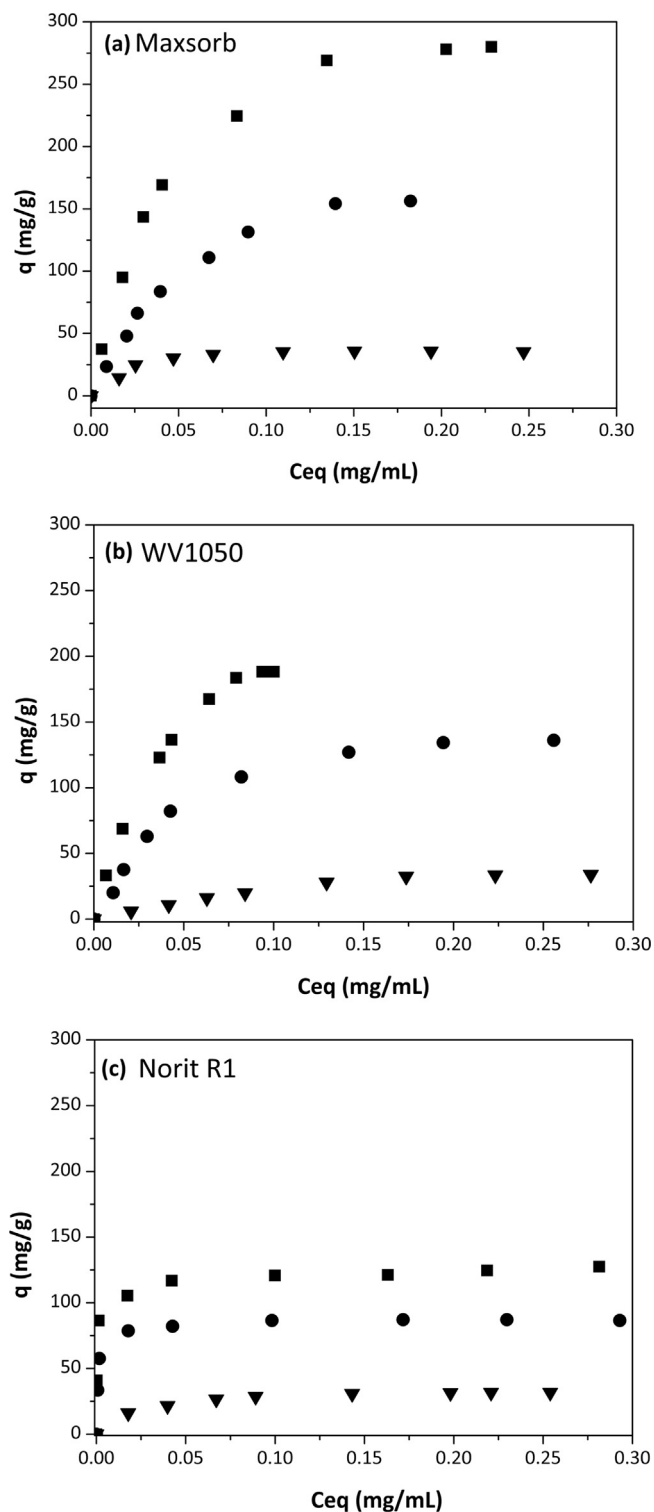


Fig. 4. Experimental equilibrium isotherms of dyes (■AB25; ●PRMX5B; ▼RR120) on carbons Maxsorb (A), WV 1050 (B), Norit R1 (C). The symbols and the error bars have similar sizes.

the large slope of the isotherm. As the WV1050 carbon has greater pore volume in the higher pore size range, its slope is smoother.

This reasoning is also valid to the Maxsorb isotherm. Maxsorb and Norit R1 has the same amount of pores in the 8.9 Å range, but Maxsorb has far more volume in the others ranges. The Maxsorb high volume in 18.5 and 27.9 Å pore ranges also explain the record amount of AB25 adsorbed by this carbon (288 mg/g).

3.3.2. PRMX-5B

This dye has a similar behavior to that of AB25 regarding the maximum amounts retained. The theoretical ratio Maxsorb:Norit and WV 1050:Norit were 3.5 and 2.6 while the experimental ratio was 2.5 and 1.7 respectively. Again, the Norit isotherm has a greater slope. Maxsorb adsorb 162 mg/g, a considerably higher amount, as was predicted by the PSDs. Based on the molecular simulation data of the selected pore, we expected that the carbons Norit, WV 1050 and Maxsorb had adsorbed similar amounts of AB25 and PRMX-5B dyes, however, the carbons adsorbed approximately 30% less (Maxsorb adsorbed 40% less). Our hypothesis to explain this result is that PRMX-5B has two sulfonic acid groups while AB25 has only one. Therefore, the PRMX-5B tendency to form dimers or trimers is superior to that of AB25 [35]. Dimers and trimers are prone to pore blockage and this would explain the decrease of the amount adsorbed. It is noteworthy that the geometry of connection between pore is not being considered, Pelekani and Snoeyink [9] showed evidences that pore network also affects dye adsorption.

3.3.3. RR120

To this dye, we obtained the most surprising experimental adsorption results. The dye RR120 batch essays showed that it adsorbs almost the same quantities on all carbons analyzed (31, 33 and 35 mg/g on Norit R1, WV1050 and Maxsorb respectively). We expected that WV1050 and Maxsorb could adsorb increased amounts. Our conclusion is that these molecules do not actually fill any pore range and adsorb only on the external surface of the activated carbon. To test this possibility we check a carbon from peach stones (Peach_0). In this carbon synthesis, the ground peach stone was only pre-washed with a 10 wt% sulfuric acid solution and submitted to one step carbonization at 450 °C under air [36]. No chemical or physical activation was done. As a result we obtain a low area carbon with only 288 m²/g, with a PSD presenting a low volume in the small pore range (Fig. S7). Experimental batch adsorption essays performed in this sample gives maximum adsorption of 30 mg/g (Fig. S8), the same adsorption amount of Norit, WV1050 and Maxsorb, confirming that the dye RR120 only adsorbs on the surface of our tested commercial carbons. The RR120 dye molecules also has a strong tendency to form dimers and possible trimers and we can expect high probability of pore blockage. The incompatibility between dye molecule and pore size indicates that conventional activated carbons are not suitable for adsorption of dye molecules in the RR120 size range.

4. Conclusions

We present an experimental collection of data between a range of dyes sizes and well-known activated carbons suited to verify the relationship between PSD and dye adsorption capacity. The experimental data were combined with molecular modeling to help interpreting the behavior of dye molecules in the activated carbon samples emphasizing the importance of the PSD.

Smaller dye molecules as the AA25, has access to the full range of pores found in conventional activated carbons. For these molecules, the correlation between adsorption capacity and its PSD seem to be independent of other factors such as geometry of interconnecting pores or surface chemistry. For intermediate size molecules such as PRMX-5B there is still a strong correlation with the PSDs but others factors such as individual potential interaction between the dye molecules have some influence. For bigger molecules with similar size of the RR120 dye, the PSD is irrelevant to predict adsorption. In this case, geometric factors and molecule–molecule interaction should be take in account. Based on our results, the carbon PSD analyses with the simplified selected pores and atomic level test with

NVT ensemble, can be a useful tool to best match a dye molecule with the available commercial activated carbons.

Acknowledgements

The authors would like to thank CNPq (Universal 2010 Process No. 474436-2010-1), CAPES, UNSL and UFC for the financial support. We would like to thank Dra. Debora A.S. Maia for kindly providing the Peach.0 sample.

Appendix A. Supplementary data

Supplementary data associated with this article can be found, in the online version, at <http://dx.doi.org/10.1016/j.colsurfa.2015.09.054>.

References

- [1] M. Iranifam, M. Zarei, A.R. Khataee, Decolorization of C.I. basic yellow 28 solution using supported ZnO nanoparticles coupled with photoelectro-Fenton process, *J. Electroanal. Chem.* 659 (1) (2011) 107–112, <http://dx.doi.org/10.1016/j.jelechem.2011.05.010>.
- [2] C. Namasivayam, D. Kavitha, Removal of congo red from water by adsorption onto activated carbon prepared from coir pith, an agricultural solid waste, *Dyes Pigments* 54 (1) (2002) 47–58, [http://dx.doi.org/10.1016/S0143-7208\(02\)00025-6](http://dx.doi.org/10.1016/S0143-7208(02)00025-6).
- [3] M.H. Karaoglu, M. Doğan, M. Alkan, Kinetic analysis of reactive blue 221 adsorption on kaolinite, *Desalination* 256 (1–3) (2010) 154–165, <http://dx.doi.org/10.1016/j.desal.2010.01.021>.
- [4] G.L. Dotto, L.A.A. Pinto, Analysis of mass transfer kinetics in the biosorption of synthetic dyes onto *Spirulina platensis* nanoparticles, *Biochem. Eng. J.* 68 (2012) 85–90, <http://dx.doi.org/10.1016/j.bej.2012.07.010>.
- [5] J.J.M. Órfão, A.I.M. Silva, J.C.V. Pereira, S.A. Barata, I.M. Fonseca, P.C.C. Faria, M.F.R. Pereira, Adsorption of a reactive dye on chemically modified activated carbons—influence of pH, *J. Colloid Interface Sci.* 296 (2) (2006) 480–489, <http://dx.doi.org/10.1016/j.jcis.2005.09.063>.
- [6] A. Rodríguez, J. García, G. Ovejero, M. Mestanza, Adsorption of anionic and cationic dyes on activated carbon from aqueous solutions: equilibrium and kinetics, *J. Hazard. Mater.* 172 (2–3) (2009) 1311–1320, <http://dx.doi.org/10.1016/j.jhazmat.2009.07.138>.
- [7] V. Singh, A.K. Sharma, D.N. Tripathi, R. Sanghi, Poly(methylmethacrylate) grafted chitosan: an efficient adsorbent for anionic azo dyes, *J. Hazard. Mater.* 161 (2–3) (2009) 955–966, <http://dx.doi.org/10.1016/j.jhazmat.2008.04.096>.
- [8] C. Pelekani, V.L. Snoeyink, Competitive adsorption between atrazine and methylene blue on activated carbon: the importance of pore size distribution, *Carbon* 38 (2000) 1423–1436.
- [9] C. Pelekani, V.L. Snoeyink, A kinetic and equilibrium study of competitive adsorption between atrazine and congo red dye on activated carbon: the importance of pore size distribution, *Carbon* 39 (2001) 25–37.
- [10] L. Li, P.A. Quinlivan, D.R.U. Knappe, Effects of activated carbon surface chemistry and pore structure on the adsorption of organic contaminants from aqueous solution, *Carbon* 40 (2002) 2085–2100.
- [11] S. Velten, D.R.U. Knappe, J. Traber, H.-P. Kaiser, U. Gunten, M. Boller, S. Meylan, Characterization of natural organic matter adsorption in granular activated carbon adsorbers, *Water Res.* 45 (2011) 3951–3959.
- [12] S.M.P. Lucena, V.A. Gomes, D.V. Gonçalves, P.G.M. Mileo, P.F.G. Silvino, Molecular simulation of the accumulation of alkanes from natural gas in carbonaceous materials, *Carbon* 61 (2013) 624–632, <http://dx.doi.org/10.1016/j.carbon.2013.05.046>.
- [13] S.M.P. Lucena, C.A.S. Paiva, P.F.G. Silvino, D.C.S. Azevedo, C.L. Cavalcante Jr., The effect of heterogeneity in the randomly etched graphite model for carbon pore size characterization, *Carbon* 48 (9) (2010) 2554–2565, <http://dx.doi.org/10.1016/j.carbon.2010.03.034>.
- [14] J.C. Alexandre de Oliveira, R.H. Lopez, S.M.P. Toso, C.L. Cavalcante, D.C.S. Azevedo, G. Zgrablich, On the influence of heterogeneity of graphene sheets in the determination of the pore size distribution of activated carbons, *Adsorption* 17 (2011) 845–851.
- [15] P.I. Ravikovitch, A. Vishnyakov, R. Russo, A.V. Neimark, Unified approach to pore size characterization of microporous carbonaceous materials from N₂, Ar, and CO₂ adsorption isotherms, *Langmuir* 16 (2000) 2311–2320.
- [16] J. Jagiello, M. Thommes, Comparison of DFT characterization methods based on N₂, Ar, CO₂, and H₂ adsorption applied to carbons with various pore size distributions, *Carbon* 42 (2004) 1227–1232.
- [17] S.J. Gregg, K.S.W. Sing, *Adsorption, Surface Area and Porosity*, Second ed., Academic Press, New York, 1982, pg 303.
- [18] F. Rouquerol, J. Rouquerol, K. Sing, *Adsorption by Powders and Porous Solids*, Academic Press, San Diego, 1999.
- [19] G. Whaba, Practical approximate solutions to linear operator equations when the data are noisy, *SIAM J. Numer. Anal.* 14 (1977) 651–667.
- [20] J.D. Wilson, Statistical approach to the solution of first-kind integral equations arising in the study of materials and their properties, *J. Mater. Sci.* 27 (1992) 3911–3924.
- [21] M.V. Szombathely, P. Brauer, M. Jaroniec, The solution of adsorption integral equations by means of the regularization method, *J. Comput. Chem.* 13 (1992) 17–32.
- [22] P.H. Merz, Determination of adsorption energy distribution by regularization and a characterization of certain adsorption isotherms, *J. Comput. Phys.* 38 (1980) 64–85.
- [23] G.M. Davies, N.A. Seaton, The effect of the choice of pore model on the characterization of the internal structure of microporous carbons using pore size distributions, *Carbon* 36 (1998) 1473–1490.
- [24] G.M. Davies, N.A. Seaton, V.S. Vassiliadis, Calculation of pore size distributions of activated carbons from adsorption isotherms, *Langmuir* 15 (1999) 8235–8245.
- [25] A.K. Rappe, W.A. Goddard, Charge equilibration for molecular dynamics simulations, *J. Phys. Chem.* 95 (1991) 3358–3363.
- [26] M.P. Tosi, Cohesion of ionic solids in the born model, *Solid State Phys.* 16 (1964) 107.
- [27] W.A. Steele, *The Interaction of Gases with Solid Surfaces*, Pergamon, New York, 1974.
- [28] M.P. Allen, D.J. Tildesley, *Computer Simulation of Liquids*, Clarendon Press Oxford, New York, 1987.
- [29] S.K. Bhatia, Density functional theory analysis of the influence of pore wall heterogeneity on adsorption in carbons, *Langmuir* 18 (2002) 6845–6856.
- [30] T.X. Nguyen, S.K. Bhatia, Probing the wall structure of nanoporous carbons using adsorption, *Langmuir* 20 (2004) 3532–3535.
- [31] T.X. Nguyen, S.K. Bhatia, Characterization of pore wall heterogeneity in nanoporous carbons using adsorption: the slit pore model revisited, *J. Phys. Chem. B* 108 (2004) 14032–14042.
- [32] Z.B. Wen, Q.T. Qu, Q. Gao, X.W. Zheng, Z.H. Hu, Y.P. Wu, et al., An activated carbon with high capacitance from carbonization of a resorcinol–formaldehyde resin, *Electrochem. Commun.* 11 (2009) 715–718.
- [33] B.B. Saha, A. Chakraborty, S. Koyama, S.-H. Yoon, I. Mochida, M. Kumja, et al., Isotherms and thermodynamics for the adsorption of *n*-butane on pitch based activated carbon, *Int. J. Heat Mass Transf.* 51 (2008) 1582–1589.
- [34] T. Otowa, R. Tanibata, M. Itoh, Production and adsorption characteristics of MAXSORB: high-surface-area active carbon, *Gas Sep. Purif.* 7 (1993) 241–245.
- [35] J.D. Hamlin, D.A.S. Phillips, A. Whiting, UV/visible spectroscopic studies of the effects of common salt and urea upon reactive dye solutions, *Dyes Pigments* 41 (1999) 137–142.
- [36] D.A.S. Maia, K. Sapag, J.P. Toso, R.H. Lopez, D.C.S. Azevedo, C.L. Cavalcante, G. Zgrablich, Characterization of activated carbons from peach stones through the mixed geometry model, *Microporous Mesoporous Mater.* 134 (2010) 181–188.